

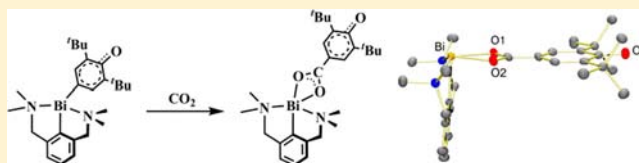
Insertion of CO₂ and COS into Bi–C Bonds: Reactivity of a Bismuth NCN Pincer Complex of an Oxyaryl Dianionic Ligand, [2,6-(Me₂NCH₂)₂C₆H₃]Bi(C₆H₂^tBu₂O)

Douglas R. Kindra, Ian J. Casely, Megan E. Fieser, Joseph W. Ziller, Filipp Furche, and William J. Evans*

Department of Chemistry, University of California, Irvine, California 92697-2025, United States

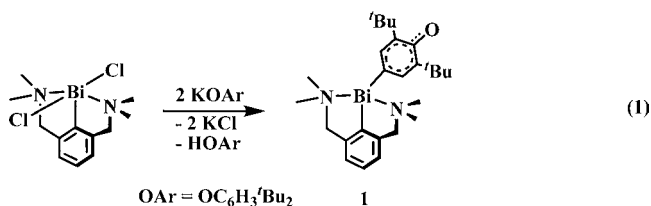
S Supporting Information

ABSTRACT: The reactivity of the unusual oxyaryl dianionic ligand, (C₆H₂^tBu₂-3,5-O-4)²⁻, in the Bi³⁺ NCN pincer complex Ar'Bi(C₆H₂^tBu₂-3,5-O-4), **1**, [Ar' = 2,6-(Me₂NCH₂)₂C₆H₃] has been explored with small molecule substrates and electrophiles. The first insertion reactions of CO₂ and COS into Bi–C bonds are observed with this oxyaryl dianionic ligand complex. These reactions generate new dianions that have quinoidal character similar to the oxyaryl dianionic ligand in **1**. The oxyarylcarboxy and oxyarylthiocarboxy dianionic ligands were identified by X-ray crystallography in Ar'Bi[O₂C(C₆H₂^tBu₂-3,5-O-4)-κ²O,O'], **2**, and Ar'Bi[OSC(C₆H₂^tBu₂-3,5-O-4)-κ²O,S], **3**, respectively. Silyl halides and pseudohalides, R₃SiX (X = Cl, CN, N₃; R = Me, Ph), react with **1** by attaching X to bismuth and R₃Si to the oxyaryl oxygen to form Ar'Bi(X)(C₆H₂^tBu₂-3,5-OSiR₃-4) complexes, a formal addition across five bonds. These react with additional R₃SiX to generate Ar'BiX₂ complexes and R₃SiOC₆H₃^tBu₂-2,6. The reaction of **1** with I₂ forms Ar'BiI₂ and the coupled quinone, 3,3',5,5'-tetra-*tert*-butyl-4,4'-diphenoquinone, by oxidative coupling.



INTRODUCTION

Recent studies of the chemistry of bismuth stabilized by the NCN phenyl pincer ligand, 2,6-(Me₂NCH₂)₂C₆H₃, Ar',^{1–7} have revealed that a new type of ligand, a dianionic oxyaryl species, (C₆H₂^tBu₂-3,5-O-4)²⁻, can be created when sterically bulky aryloxy ligands react with Ar'BiCl₂, eq 1.⁸ In contrast to

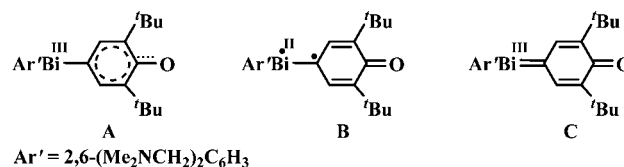


reactions with smaller aryloxy anions that make the three-ligand complexes Ar'Bi(OC₆H₃R₂)₂ (R = Me, ^tPr), Ar'BiCl₂ reacts with KOC₆H₂^tBu₂-2,6 to form a product with only two ligands, Ar'Bi(C₆H₂^tBu₂-3,5-O-4), **1**. This reaction involves C–H bond activation and formation of HOC₆H₃^tBu₂-2,6 as a byproduct.

NMR and IR spectroscopy, crystallographic studies, and DFT calculations indicate that complex **1** is a Bi³⁺ complex with an oxyaryl dianionic ligand that has ring C–C and C–O distances consistent with considerable quinoidal character.⁸ This complex is best described by structure **A**, Scheme 1, rather than as a Bi²⁺ complex of a radical, structure **B**, or a complex with a Bi=C(aryl) double bond, structure **C**.

We describe here the reaction chemistry of this unusual oxyaryl dianionic ligand complex. Complex **1** reacts with CO₂ and COS to provide the first examples of insertion of these

Scheme 1. Possible Bonding Arrangements for **1**, the Bismuth NCN Pincer Complex of the Oxyaryl Dianionic Ligand (C₆H₂^tBu₂-3,5-O-4)²⁻



small molecule substrates into a Bi–C bond. These reactions generate two new dianionic ligands with quinoidal characteristics. Reactions of silyl halides and pseudohalides are also reported in which Me₃Si–X formally adds over five bonds to the bismuth and oxygen components of complex **1**.

EXPERIMENTAL DETAILS

All manipulations and syntheses described below were conducted with the rigorous exclusion of air and water using standard Schlenk line and glovebox techniques under an argon or dinitrogen atmosphere. Solvents were sparged with UHP argon and dried by passage through columns containing Q-5 and molecular sieves prior to use. Deuterated NMR solvents were dried over NaK alloy, degassed by three freeze–pump–thaw cycles, and vacuum transferred before use. ¹H NMR spectra were recorded on Bruker DR400, GN500, or CRYOS00 MHz spectrometers (¹³C NMR spectra on the 500 MHz spectrometer operating at 125 MHz, ¹⁹F NMR spectra on the DR400 spectrometer operating at 375 MHz) at 298 K unless otherwise stated and referenced internally to residual protio-solvent resonances. GC–MS

Received: March 28, 2013

Published: April 26, 2013

spectra were collected on a ThermoTrace MS and GC–MS instrument. Elemental analyses were conducted on a Perkin-Elmer 2400 Series II CHNS elemental analyzer. $\text{KOC}_6\text{H}_3^t\text{Bu}_2$ -2,6 and $\text{KOC}_6\text{H}_2^t\text{Bu}_2$ -2,6-Me-4 were synthesized via an adaptation of a literature procedure by treatment of the parent phenol with 1 equiv of $\text{KN}(\text{SiMe}_3)_2$ in toluene, followed by filtration of the resulting white solid, and washing with hexane.⁹ $[\text{Et}_3\text{NH}][\text{BPh}_4]$ was synthesized by treatment of $[\text{Et}_3\text{NH}][\text{Cl}]$ with NaBPh_4 in water, followed by filtration and drying under a high vacuum (10^{-5} Torr) for 48 h.⁸ CO_2 (99.98%), $^{13}\text{C}\text{O}_2$ (99%), and COS (96+ %) were purchased from Airgas, Cambridge Isotope Laboratories, and Matheson, respectively. Phenol reagents were sublimed prior to use. Me_3SiN_3 and Me_3SiCN (Sigma-Aldrich) were distilled under argon before use. Me_3SiCl (Alfa Aesar, 98+%) and Ph_3SiCl (Sigma-Aldrich, 97%) were received packed under argon and used without further purification. $\text{Ar}^t\text{Bi}(\text{OC}_6\text{H}_3\text{Me}_2$ -2,6)₂ was prepared according to the literature.⁸

[2,6-(Me₂NCH₂)₂C₆H₃]Bi(C₆H₂^tBu₂-3,5-O-4), 1. This procedure is an improved route to **1** compared to that in the literature.⁸ A white opaque suspension of $\text{KOC}_6\text{H}_3^t\text{Bu}_2$ -2,6 (1.16 g, 4.74 mmol) in THF (15 mL) was slowly added by pipet into a stirred solution of Ar^tBiCl_2 (1.00 g, 2.31 mmol) in THF (70 mL). The cloudy white mixture turned yellow, then orange, and finally a dark red color after mixing. After 4 h of stirring, the reaction solution was centrifuged and filtered to remove insoluble material. Addition of hexane (300 mL) to the stirred filtrate generated an orange insoluble material that was filtered, washed with additional hexane, and dried under a vacuum. This crude product was dissolved in THF and allowed to precipitate with the addition of hexane. This reduced the amount of $\text{HOC}_6\text{H}_3^t\text{Bu}_2$ -2,6 byproduct and caused the color to become bright orange. This process was repeated 3 times to give analytically pure bright orange **1** (850 mg, 61%). ¹H NMR (500 MHz, acetonitrile-*d*₃): δ 7.51 [m, 5H, (Me₂NCH₂)₂C₆H₃ and C₆H₂^tBu₂O], 3.88 [d, ²J_{HH} = 14.7 Hz, 2H, (Me₂NCH₂)₂C₆H₃], 3.76 [d, ²J_{HH} = 14.7 Hz, 2H, (Me₂NCH₂)₂C₆H₃], 2.67 [s, 6H, (Me₂NCH₂)₂C₆H₃], 2.26 [s, 6H, (Me₂NCH₂)₂C₆H₃], 1.24 [s, 18H, C₆H₂^tBu₂O]. ¹³C NMR (125 MHz, acetonitrile-*d*₃): δ 182.7 [i-(Me₂NCH₂)₂C₆H₃], 174.5 [i-C₆H₂^tBu₂O], 159.0 and 139.6 [C₆H₂^tBu₂O], 149.7 [o-(Me₂NCH₂)₂C₆H₃], 134.5, 129.0, and 127.7 [m- and p-(Me₂NCH₂)₂C₆H₃ and C₆H₂^tBu₂O], 67.2 [(Me₂NCH₂)₂C₆H₃], 46.5 [(Me₂NCH₂)₂C₆H₃], 46.4 [(Me₂NCH₂)₂C₆H₃], 34.9 [q-C₆H₂(CMe₃)₂O], 29.1 [C₆H₂(CMe₃)₂O]. IR: 3045w, 2991w, 2943m, 2894m, 2840w, 2797w, 1554s, 1477s, 1432s, 1374m, 1354m, 1333m, 1300w, 1254m, 1202w, 1173w, 1127w, 1091s, 1034w, 1005m, 885w, 840s, 803w, 775w, 709w, 530w, 444m cm⁻¹. Anal. Calcd for C₂₆H₃₉N₂O₂Bi: C, 51.64; H, 6.51; N, 4.63. Found: C, 52.07; H, 6.99; N, 4.35.

[2,6-(Me₂NCH₂)₂C₆H₃]Bi[O₂C(C₆H₂^tBu₂-3-5-O-4)-κ²O,O'], 2. A 100 mL sealable side arm Schlenk flask was charged with bright orange **1** (130 mg, 0.22 mmol). Addition of acetonitrile (10 mL) formed a red solution. The flask was placed on a high vacuum line, degassed, and charged with 1 atm of carbon dioxide. After stirring at room temperature for 1 h, a yellow precipitate formed. The flask was degassed with three freeze–pump–thaw cycles and transferred to an argon-filled glovebox. The reaction mixture was concentrated under a vacuum, and the solids were collected via centrifugation, washed with hexane, and dried under a vacuum giving **2** as a yellow powder (102 mg, 73%). X-ray quality crystals were grown from a saturated acetonitrile solution at –30 °C. ¹H NMR (500 MHz, acetonitrile-*d*₃): δ 7.70 [d, ²J_{HH} = 6.99 Hz, 2H, (Me₂NCH₂)₂C₆H₃], 7.64 [s, 2H, O₂C(C₆H₂^tBu₂O)], 7.52 [t, 1H, ³J_{HH} = 14.8 Hz, (Me₂NCH₂)₂C₆H₃], 4.29 [s, 4H, (Me₂NCH₂)₂C₆H₃], 2.68 [s, 12H, (Me₂NCH₂)₂C₆H₃], 1.36 [s, 18H, O₂C(C₆H₂^tBu₂O)]. ¹³C NMR (125 MHz, acetonitrile-*d*₃): δ 130.6, 129.1, 127.8, and 126.2 [m- and p-(Me₂NCH₂)₂C₆H₃ and O₂C(C₆H₂^tBu₂O)], 68.7 [(Me₂NCH₂)₂C₆H₃], 46.3 [(Me₂NCH₂)₂C₆H₃], 35.6 [q-O₂C(C₆H₂(CMe₃)₂O)], 30.7 [O₂C(C₆H₂(CMe₃)₂O)]. IR: 3631w, 2951s, 2794w, 1665w, 1591s, 1546m, 1468s, 1424s, 1322s, 1010m, 841s, 694m cm⁻¹. Anal. Calcd for C₂₇H₃₉N₂O₃Bi: C, 50.00; H, 6.06; N, 4.32. Found: C, 49.70; H, 5.93; N, 4.23. UV–Vis (MeCN): λ_{max} (nm), ε (M⁻¹ cm⁻¹) 357, 15600; 249, 18600.

[2,6-(Me₂NCH₂)₂C₆H₃]Bi[O₂¹³C(C₆H₂^tBu₂-3-5-O-4)-κ²O,O'], 2-¹³C. The ¹³C analogue of **2** was prepared analogously from ¹³CO₂ (90 mg, 73%). ¹³C NMR (125 MHz, acetonitrile-*d*₃): δ 175.8 [O₂¹³C(C₆H₂^tBu₂O)] 130.6, 129.1, 127.8, and 126.2 [m- and p-(Me₂NCH₂)₂C₆H₃ and O₂C(C₆H₂^tBu₂O)], 68.7 [(Me₂NCH₂)₂C₆H₃], 46.3 [(Me₂NCH₂)₂C₆H₃], 35.6 [q-O₂C(C₆H₂(CMe₃)₂O)], 30.7 [O₂C(C₆H₂(CMe₃)₂O)]. IR: 3631w, 2951s, 2794w, 1665w, 1591s, 1523m (calcd 1512), 1468s, 1424s, 1305s (calcd 1293), 1010m, 841s, 694m cm⁻¹.

[2,6-(Me₂NCH₂)₂C₆H₃]Bi[OSC(C₆H₂^tBu₂-3-5-O-4)-κ²O,S], 3. A 100 mL sealable side arm Schlenk flask was charged with bright orange **1** (150 mg, 0.25 mmol). Addition of acetonitrile (15 mL) formed a red solution. The flask was placed on a high vacuum line, degassed, and charged with 1 atm of carbonyl sulfide (COS) gas. After stirring at room temperature for 1 h, an orange precipitate formed. The flask was degassed with three freeze–pump–thaw cycles and moved into a nitrogen-filled glovebox. The solids were collected via centrifugation, washed with hexane, and dried under a vacuum giving **3** as an orange powder (108 mg, 65%). X-ray quality crystals were grown from a saturated acetonitrile solution at –30 °C. ¹H NMR (500 MHz, acetonitrile-*d*₃): δ 7.70 [d, ²J_{HH} = 7.34 Hz, 2H, (Me₂NCH₂)₂C₆H₃], 7.54 [t, ³J_{HH} = 14.8 Hz, 1H, (Me₂NCH₂)₂C₆H₃], 7.48 [s, 2H, OSC(C₆H₂^tBu₂O)], 4.29 [s, 4H, (Me₂NCH₂)₂C₆H₃], 2.67 [br s, 12H, (Me₂NCH₂)₂C₆H₃], 1.28 [s, 18H, OSC(C₆H₂^tBu₂O)]. ¹³C NMR (125 MHz, acetonitrile-*d*₃): δ 130.8, 129.6, 127.4, and 126.3 [m- and p-(Me₂NCH₂)₂C₆H₃ and OSC(C₆H₂^tBu₂O)], 69.8 [(Me₂NCH₂)₂C₆H₃], 48.0 [br s, (Me₂NCH₂)₂C₆H₃], 36.5 [q-OSC(C₆H₂(CMe₃)₂O)], 30.3 [OSC(C₆H₂(CMe₃)₂O)]. IR: 2957s, 2816s, 2780s, 1735s, 1597m, 1448s, 1362m, 1296w, 1227s, 1185s, 1097s, 1019s, 843s, 792m, 758s, 713w, 618w cm⁻¹. Anal. Calcd for C₂₇H₃₉BiN₂O₂S·CH₃CN: C, 49.34; H, 6.00; N, 5.96. Found: C, 49.30; H, 5.89; N, 5.47. UV–Vis (MeCN): λ_{max} (nm), ε (M⁻¹ cm⁻¹) 396, 38300; 270, 14400.

{[2,6-(Me₂NCH₂)₂C₆H₃]Bi[O₂C(C₆H₂^tBu₂-3-5-OH-4)-κ²O,O']}]·[BPh₄], 5. A colorless solution of $[\text{Et}_3\text{NH}][\text{BPh}_4]$ (130 mg, 0.31 mmol) in THF (12 mL) was slowly added to a stirred yellow suspension of **2** (190 mg, 0.29 mmol) in THF (5 mL). The reaction mixture quickly became a very pale yellow solution. After stirring at room temperature for 1 h, the solvent was removed under a vacuum yielding a fluffy off-white powder. The crude product was further purified by recrystallization in acetonitrile at –30 °C yielding white needle-shaped crystals of **5** (254 mg, 88%). ¹H NMR (500 MHz, acetonitrile-*d*₃): δ 7.88 [d, ²J_{HH} = 7.50 Hz, 2H, (Me₂NCH₂)₂C₆H₃], 7.78 [s, 2H, O₂C(C₆H₂^tBu₂OH)], 7.65 [t, ³J_{HH} = 15.0 Hz, 1H, (Me₂NCH₂)₂C₆H₃], 7.29 [m, 8H, *m*-BPh₄], 7.01 [m, 8H, *o*-BPh₄], 6.84 [m, 4H, *p*-BPh₄], 6.13 [s, 1H, O₂C(C₆H₂^tBu₂OH)], 4.46 [s, 4H, (Me₂NCH₂)₂C₆H₃], 2.76 [s, 12H, (Me₂NCH₂)₂C₆H₃], 1.39 [s, 18H, O₂C(C₆H₂^tBu₂OH)]. ¹³C NMR (125 MHz, acetonitrile-*d*₃): δ 163.8 [BPh₄], 155.4 [O₂C(C₆H₂^tBu₂OH)], 137.7 [BPh₄], 131.9, 129.5, 128.4, and 126.6 [m- and p-(Me₂NCH₂)₂C₆H₃ and O₂C(C₆H₂^tBu₂OH)], 122.8 [BPh₄], 69.1 [(Me₂NCH₂)₂C₆H₃], 47.1 [(Me₂NCH₂)₂C₆H₃], 35.2 [q-O₂C(C₆H₂(CMe₃)₂OH)], 30.2 [O₂C(C₆H₂(CMe₃)₂OH)]. IR: 3620s, 3414br, 3057s, 2958s, 2872s, 2798m, 1948w, 1887w, 1817w, 1598s, 1562s, 1476s, 1388s, 1239s, 1117s, 1004s, 889m, 836s, 733s, 707s, 612s cm⁻¹. Anal. Calcd for C₅₀H₅₈BN₂O₃Bi: C, 62.90; H, 6.12; N, 2.93. Found: C, 63.19; H, 5.99; N, 2.91.

[2,6-(Me₂NCH₂)₂C₆H₃]Bi(Cl)(C₆H₂^tBu₂-3,5-Osime₃-4), 6. A scintillation vial was charged with bright orange **1** (100 mg, 0.17 mmol). Addition of THF (10 mL) formed a dark red solution. When a colorless solution of Me_3SiCl (22 μL, 0.17 mmol) in THF (10 mL) was added to the reaction vessel, the mixture instantly turned clear and colorless. After 3 h, the mixture was an off-white suspension and was stored overnight at –30 °C to precipitate further product. The supernatant was decanted, and the white solids were washed with cold THF and collected by centrifugation. The white powder was dried under a vacuum to yield analytically pure **6** (101 mg, 86%). ¹H NMR (500 MHz, acetonitrile-*d*₃): δ 8.02 [s, 2H, C₆H₂^tBu₂OSiMe₃], 7.59 [s, 3H, *m*- and *p*-(Me₂NCH₂)₂C₆H₃], 4.13 [d, ²J_{HH} = 14.8 Hz, 2H, (Me₂NCH₂)₂C₆H₃], 3.72 [d, ²J_{HH} = 14.8 Hz, 2H, (Me₂NCH₂)₂C₆H₃], 2.52 [br s, 12H, (Me₂NCH₂)₂C₆H₃], 1.28 [s, 18H, C₆H₂^tBu₂OSiMe₃], 0.32 [s, 9H, C₆H₂^tBu₂OSiMe₃]. ¹³C NMR (125 MHz, acetonitrile-*d*₃):

δ 188.4 [*i*-(Me₂NCH₂)₂C₆H₃], 176.5 [*i*-C₆H₂^tBu₂OSiMe₃], 154.0 and 143.9 [C₆H₂^tBu₂OSiMe₃], 150.6 [*o*-(Me₂NCH₂)₂C₆H₃], 136.4 [C₆H₂^tBu₂OSiMe₃], 129.3 [*p*-(Me₂NCH₂)₂C₆H₃], 127.8 [*m*-(Me₂NCH₂)₂C₆H₃], 67.8 [(Me₂NCH₂)₂C₆H₃], 47.0 [(Me₂NCH₂)₂C₆H₃], 35.3 [*q*-C₆H₂(CMe₃)₂OSiMe₃], 30.8 [C₆H₂(CMe₃)₂OSiMe₃], 2.53 [C₆H₂^tBu₂OSiMe₃]. IR: 3037w, 2956m, 2903m, 2869m, 2835w, 2793w, 2711w, 1579w, 1551w, 1469m, 1451m, 1417m, 1392m, 1361m, 1256m, 1231m, 1202m, 1176w, 1150w, 1131m, 1070w, 1034w, 1003m, 910m, 843s, 770m, 710w, 676w, 637w, 562w, 528w, 481w, 451w, 412w cm⁻¹. Anal. Calcd for C₂₉H₄₈BiClN₂O₂Si: C, 48.83; H, 6.80; N, 3.93. Found: C, 48.93; H, 6.77; N, 3.84.

[2,6-(Me₂NCH₂)₂C₆H₃]Bi(Cl)(C₆H₂^tBu₂-3,5-OSiPh₃-4), 7. A scintillation vial was charged with bright orange **1** (100 mg, 0.17 mmol). Addition of THF (10 mL) formed a dark red solution. Addition of Ph₃SiCl (49 mg, 0.17 mmol) in THF (12 mL) caused no immediate change in appearance. After stirring overnight, the reaction mixture became a yellow suspension. The solids were collected by centrifugation and washed three times with THF to afford **7** as a white solid (99 mg, 67%). ¹H NMR (500 MHz, acetonitrile-*d*₃): δ 7.85 [s, 2H, C₆H₂^tBu₂OSiPh₃], 7.61 [s, 3H, (Me₂NCH₂)₂C₆H₃], 7.53 [t, ³J_{HH} = 8.03 Hz, 6H, *o*-C₆H₂^tBu₂OSiPh₃], 7.45 [m, 3H, *p*-C₆H₂^tBu₂OSiPh₃], 7.33 [t, ³J_{HH} = 15.3 Hz, 6H, *m*-C₆H₂^tBu₂OSiPh₃], 4.14 [d, ²J_{HH} = 15.0 Hz, 2H, (Me₂NCH₂)₂C₆H₃], 3.82 [d, ²J_{HH} = 15.0 Hz, 2H, (Me₂NCH₂)₂C₆H₃], 2.60 [br s, 12H, (Me₂NCH₂)₂C₆H₃], 0.91 [s, 18H, C₆H₂^tBu₂OSiPh₃]. ¹³C NMR (125 MHz, acetonitrile-*d*₃): δ 187.3 [*i*-(Me₂NCH₂)₂C₆H₃], 176.5 [*i*-C₆H₂^tBu₂OSiPh₃], 154.7 and 145.8 [C₆H₂^tBu₂OSiPh₃], 151.7 [*o*-(Me₂NCH₂)₂C₆H₃], 137.9 [C₆H₂^tBu₂OSiPh₃], 137.4 [*o*-C₆H₂^tBu₂OSiPh₃], 135.4 [C₆H₂^tBu₂OSiPh₃], 131.5 [*m*-C₆H₂^tBu₂OSiPh₃], 131.0 [*p*-C₆H₂^tBu₂OSiPh₃], 129.4 [*p*-(Me₂NCH₂)₂C₆H₃], 129.1 [*m*-(Me₂NCH₂)₂C₆H₃], 69.0 [(Me₂NCH₂)₂C₆H₃], 48.4 [(Me₂NCH₂)₂C₆H₃], 37.2 [*q*-C₆H₂(CMe₃)₂OSiPh₃], 32.8 [C₆H₂(CMe₃)₂OSiPh₃]. IR: 2955m, 2866m, 1589w, 1468m, 1415s, 1223s, 1114s, 1002m, 907m, 842s, 774m, 742m, 701s, 573w, 510s, 453w cm⁻¹. Anal. Calcd for C₄₄H₅₄BiClN₂O₂Si: C, 58.76; H, 6.05; N, 3.11. Found: C, 57.65; H, 6.41; N, 3.11.

{[2,6-(Me₂NCH₂)₂C₆H₃]Bi(C₆H₂^tBu₂-3,5-OSiMe₃-4)}{CF₃SO₃}, 8. A stirred white mixture of **6** (81 mg, 0.11 mmol) in THF (8 mL) rapidly turned clear and colorless upon the addition of AgOTf (31 mg, 0.12 mmol) in THF (3 mL). Subsequently, slow formation of a white precipitate occurred. After stirring overnight, the reaction mixture was centrifuged to remove off-white insoluble material consistent with silver chloride. The solvent was removed from the colorless supernatant under a vacuum to give **8** as a white powder (84 mg, 89%). X-ray quality crystals were grown from a saturated acetonitrile solution at -30 °C. ¹H NMR (500 MHz, acetonitrile-*d*₃): δ 7.91 [s, 2H, C₆H₂^tBu₂OSiMe₃], 7.64 [s, 3H, (Me₂NCH₂)₂C₆H₃], 4.06 [d, ²J_{HH} = 15.0 Hz, 2H, (Me₂NCH₂)₂C₆H₃], 3.77 [d, ²J_{HH} = 15.0 Hz, 2H, (Me₂NCH₂)₂C₆H₃], 2.75 [s, 6H, (Me₂NCH₂)₂C₆H₃], 2.25 [s, 6H, (Me₂NCH₂)₂C₆H₃], 1.29 [s, 18H, C₆H₂^tBu₂OSiMe₃], 0.33 [s, 9H, C₆H₂^tBu₂OSiMe₃]. ¹³C NMR (125 MHz, acetonitrile-*d*₃): δ 186.5 [*i*-(Me₂NCH₂)₂C₆H₃], 174.2 [*i*-C₆H₂^tBu₂OSiMe₃], 155.8 [C₆H₂^tBu₂OSiMe₃], 151.7 [*o*-(Me₂NCH₂)₂C₆H₃], 145.5 [C₆H₂^tBu₂OSiMe₃], 137.3 [C₆H₂^tBu₂OSiMe₃], 131.1 [(Me₂NCH₂)₂C₆H₃], 129.5 [(Me₂NCH₂)₂C₆H₃], 68.7 [(Me₂NCH₂)₂C₆H₃], 48.3 [(Me₂NCH₂)₂C₆H₃], 36.6 [*q*-C₆H₂(CMe₃)₂OSiMe₃], 32.0 [C₆H₂(CMe₃)₂OSiMe₃], 3.6 [C₆H₂^tBu₂OSiMe₃]. ¹⁹F NMR (375 MHz, acetonitrile-*d*₃): δ -79.36 [s, 3F, CF₃SO₃]. IR: 2959m, 2918m, 2874m, 1470m, 1416m, 1393m, 1266s, 1236s, 1156m, 1031s, 913m, 844s, 780w, 637s cm⁻¹. Anal. Calcd. for C₃₀H₄₈BiF₃N₂O₄Si: C, 43.58; H, 5.85; N, 3.39. Found: C, 43.15; H, 5.74; N, 3.85.

[2,6-(Me₂NCH₂)₂C₆H₃]Bi(CN)(C₆H₂^tBu₂-3,5-OSiMe₃-4), 9. Me₃SiCN (10 μ L, 0.08 mmol) dissolved in THF (2 mL) was added to a dark red solution of **1** (50 mg, 0.08 mmol) in THF (8 mL). The reaction mixture turned light yellow within 2 min of addition. After stirring for 30 min at ambient temperature, the reaction mixture was filtered, and the solvent was removed under a vacuum leaving orange-yellow solids (48 mg). ¹H NMR spectroscopy showed a complex

mixture of **1**, **9**, and [2,6-(Me₂NCH₂)₂C₆H₃]Bi(CN)₂, **10**. A small amount of colorless X-ray quality crystals of **9** grew at -30 °C from a saturated acetonitrile solution of this crude solid. ¹H NMR (500 MHz, acetonitrile-*d*₃): δ 8.01 [s, 2H, C₆H₂^tBu₂OSiMe₃], 7.38 [s, 3H, *m*- and *p*-(Me₂NCH₂)₂C₆H₃], 3.85 [br s, 2H, (Me₂NCH₂)₂C₆H₃], 3.35 [br s, 2H, (Me₂NCH₂)₂C₆H₃], 2.19 [s, 12H, (Me₂NCH₂)₂C₆H₃], 1.31 [s, 18H, C₆H₂^tBu₂OSiMe₃], 0.36 [s, 9H, C₆H₂^tBu₂OSiMe₃]. ¹³C NMR (125 MHz, acetonitrile-*d*₃): δ 174.1 [*i*-C₆H₂^tBu₂OSiMe₃], 165.9 [CN], 152.6 and 142.7 [C₆H₂^tBu₂OSiMe₃], 150.0 [*o*-(Me₂NCH₂)₂C₆H₃], 136.4 [C₆H₂^tBu₂OSiMe₃], 128.51 [*p*-(Me₂NCH₂)₂C₆H₃], 128.19 [*m*-(Me₂NCH₂)₂C₆H₃], 67.0 [(Me₂NCH₂)₂C₆H₃], 44.1 [(Me₂NCH₂)₂C₆H₃], 35.1 [*q*-C₆H₂(CMe₃)₂OSiMe₃], 30.8 [C₆H₂(CMe₃)₂OSiMe₃], 2.70 [C₆H₂^tBu₂OSiMe₃].

Reaction of 1 with Excess Me₃SiCl. Me₃SiCl (32 μ L, 0.25 mmol) was added by microsyringe to a stirred dark red solution of **1** (50 mg, 0.08 mmol) in THF (5 mL). The reaction mixture immediately became colorless and was stirred for 12 h. After solvent removal, the resulting white solid (52 mg) was stirred in hexane (5 mL) for 30 min, and the insoluble material was collected by centrifugation to yield an off white solid (20 mg) that was determined to be the known dichloride Ar'BiCl₂¹ by ¹H and ¹³C NMR spectroscopy. Solvent was removed from the mother liquor under reduced pressure affording a white solid determined to be Me₃SiOC₆H₃^tBu₂-2,6¹⁰ (7 mg) by ¹H NMR spectroscopy and GC-MS.

Reaction of 6 with KOC₆H₃^tBu₂-2,6. A cloudy white mixture of **6** (90 mg, 0.13 mmol) in THF (8 mL) immediately turned dark red upon the addition of KOC₆H₃^tBu₂-2,6 (32 mg, 0.13 mmol). After stirring overnight, the solvent was removed under reduced pressure, and the crude orange solid was stirred in hexane (8 mL) for 2 h. The mixture was centrifuged to recover orange solids (75 mg) that were identified as **1** by ¹H NMR spectroscopy. Hexane was removed from the supernatant under a vacuum to yield an off-white solid that was identified by ¹H NMR spectroscopy and GC-MS as (2,6-di-*tert*-butylphenoxy)trimethylsilane¹⁰ (35 mg, 97%).

Reaction of 6 with KOC₆H₃^tBu₂-2,6-Me-4. A cloudy white mixture of **6** (60 mg, 0.08 mmol) in THF (8 mL) immediately turned dark red upon the addition of KOC₆H₃^tBu₂-2,6-Me-4 (22 mg, 0.08 mmol) in THF (3 mL). After stirring for 3 h, the solvent was removed under reduced pressure, and the crude orange solid was stirred in hexane (10 mL) for 15 min. The mixture was then centrifuged to recover orange solids (35 mg) that were identified as **1** by ¹H NMR spectroscopy. The hexane was removed from the supernatant under a vacuum to yield a white solid that was identified by ¹H NMR and GC-MS as (2,6-di-*tert*-butyl-4-methylphenoxy)trimethylsilane¹¹ (22 mg, 94%).

[2,6-(Me₂NCH₂)₂C₆H₃]Bi(CN)₂, 10. Neat Me₃SiCN (24 μ L, 0.19 mmol) was added via microsyringe to a stirred yellow solution of Ar'Bi(OC₆H₃Me₂-2,6)₂ (50 mg, 0.08 mmol) in THF (5 mL). The yellow color faded, and a white precipitate began to form over 5 min. Stirring was continued for 1 h, and hexane (5 mL) was added. The mixture was filtered, and the filtrate was washed with a 1:1 THF/hexane (5 mL) mixture and dried under reduced pressure to afford **10** as a white solid (29 mg, 82%). Single crystals were grown from a concentrated MeCN solution stored at -30 °C overnight. ¹H NMR at 298 K (500 MHz, acetonitrile-*d*₃): δ 7.60 [d, ²J_{HH} = 7.5 Hz, 2H, *m*-(Me₂NCH₂)₂C₆H₃], 7.49 [t, ³J_{HH} = 7.5 Hz, 1H, *p*-(Me₂NCH₂)₂C₆H₃], 4.41 [br s, 2H, (Me₂NCH₂)₂C₆H₃], 4.04 [br s, 2H, (Me₂NCH₂)₂C₆H₃], 2.81 [br s, 6H, (Me₂NCH₂)₂C₆H₃], 2.00 [br s, 6H, (Me₂NCH₂)₂C₆H₃]. ¹³C NMR (125 MHz, acetonitrile-*d*₃): δ 152.1 [*o*-(Me₂NCH₂)₂C₆H₃], 129.7 [*p*-(Me₂NCH₂)₂C₆H₃], 128.7 [*m*-(Me₂NCH₂)₂C₆H₃], 67.6 [(Me₂NCH₂)₂C₆H₃], 45.5 [br s, (Me₂NCH₂)₂C₆H₃], 41.4 [br s, (Me₂NCH₂)₂C₆H₃]. IR: 3046w, 2988w, 2967w, 2871m, 2834m, 2802m, 2782w, 2133m, 1579w, 1474m, 1454m, 1401w, 1359w, 1275w, 1253m, 1230w, 1212w, 1174w, 1147w, 1098w, 1036m, 1010s, 970w, 894w, 842s, 794m, 765m, 708w, 526w, 467w, 437w cm⁻¹. Anal. Calcd for C₁₄H₁₉BiN₄: C, 37.17; H, 4.24; N, 12.38. Found: C, 37.28; H, 4.08; N, 12.22.

The mother liquors isolated from the syntheses of Ar'Bi(CN)₂, **10**, and Ar'Bi(N₃)₂, **11**, via this Ar'Bi(OC₆H₃Me₂-2,6)₂-based route were

Table 1. X-ray Data Collection Parameters for [2,6-(Me₂NCH₂)₂C₆H₃]Bi[O₂C(C₆H₂^tBu₂-3-5-O-4)-κ²O,O'], **2**, [2,6-(Me₂NCH₂)₂C₆H₃]Bi[OSC(C₆H₂^tBu₂-3-5-O-4)-κ²O,S], **3**, {[2,6-(Me₂NCH₂)₂C₆H₃]Bi(C₆H₂^tBu₂-3,5-OSiMe₃-4)}{CF₃SO₃}, **8**, [2,6-(Me₂NCH₂)₂C₆H₃]Bi(CN)(C₆H₂^tBu₂-3,5-OSiMe₃-4), **9**, and [2,6-(Me₂NCH₂)₂C₆H₃]Bi(N₃)₂, **11**

	2	3	8	9	11
empirical formula	C ₂₇ H ₃₉ BiN ₂ O ₃ ·CH ₃ CN	C ₂₇ H ₃₉ BiN ₂ O ₂ S	C ₃₀ H ₄₈ BiF ₃ N ₂ O ₄ SSi·CH ₃ CN	C ₃₀ H ₄₈ BiN ₃ O ₃ Si	C ₁₂ H ₁₉ BiN ₈ ·CH ₃ CN
formula weight	689.64	664.64	867.88	703.78	525.39
T (K)	88(2)	88(2)	143(2) K	93(2)	88(2)
crystal system	monoclinic	monoclinic	orthorhombic	triclinic	triclinic
space group	P2 ₁ /c	P2 ₁ /n	Pbca	P $\bar{1}$	P $\bar{1}$
a (Å)	12.7738(6)	13.2358(5)	12.0702(7)	12.9129(7)	8.2299(5)
b (Å)	13.9744(7)	17.3249(7)	16.4669(9)	14.9962(8)	9.5398(6)
c (Å)	17.9010(8)	13.3003(5)	37.181(2)	17.9034(10)	12.9942(9)
α (deg)	90	90	90	101.3228(6)	108.9940(6)
β (deg)	106.3798(5)	116.1287(4)	90	101.2366(6)	101.4449(6)
γ (deg)	90	90	90	98.9213(6)	102.6115(6)
volume Å ³	3065.7(3)	2738.20(18)	7390.0(7)	3266.2(3)	900.33(10)
Z	4	4	8	4	2
ρ _{calcd} (Mg/m ³)	1.494	1.612	1.560	1.431	1.938
μ (mm ⁻¹)	5.782	6.540	4.913	5.459	9.808
R1 ^a [I > 2.0σ(I)]	0.0220	0.0163	0.0177	0.0167	0.0123
wR2 ^a (all data)	0.0503	0.0380	0.0401	0.0385	0.0296

^aDefinitions: R1 = Σ(|F_o| - |F_c|)/Σ|F_o|, wR2 = [Σ[w(F_o² - F_c²)²]/Σ[w(F_o²)²]^{1/2}.

dried to yield off white solids identified as (2,6-dimethylphenoxy)-trimethylsilane.¹²

[2,6-(Me₂NCH₂)₂C₆H₃]Bi(N₃)₂, **11**, from **1**. Neat Me₃SiN₃ (28 μL, 0.21 mmol) was added via microsyringe to a stirred dark red solution of **1** (55 mg, 0.09 mmol) in THF (5 mL). The red color faded, and a white precipitate began to form over 5 min. Stirring was continued for 1 h, and hexane (5 mL) was added. The solids were collected by filtration, washed with a 1:1 THF/hexane mixture (5 mL), and dried under reduced pressure to afford **11** as a white solid (40 mg, 96%). ¹H NMR (500 MHz, acetonitrile-*d*₃): δ 7.79 [d, ²J_{HH} = 7.5 Hz, 2H, *m*-(Me₂NCH₂)₂C₆H₃], 7.60 [t, ³J_{HH} = 7.5 Hz, 1H, *p*-(Me₂NCH₂)₂C₆H₃], 4.31 [s, 4H, (Me₂NCH₂)₂C₆H₃], 2.82 [s, 12H, (Me₂NCH₂)₂C₆H₃]. ¹³C NMR (125 MHz, acetonitrile-*d*₃): δ 151.9 [*o*-(Me₂NCH₂)₂C₆H₃], 129.5 [*p*-(Me₂NCH₂)₂C₆H₃], 128.4 [*m*-(Me₂NCH₂)₂C₆H₃], 67.8 [(Me₂NCH₂)₂C₆H₃], 45.5 [(Me₂NCH₂)₂C₆H₃]. IR: 3046w, 2998w, 2965w, 2889w, 2864w, 2829w, 2786w, 2033vs, 2012vs, 1578w, 1453m, 1423m, 1401w, 1352w, 1312m, 1263m, 1227w, 1211w, 1172w, 1158w, 1088w, 1029m, 999m, 986m, 955w, 911w, 841s, 782m, 708w, 638w, 613w, 480w, 454m cm⁻¹. Anal. Calcd for C₁₂H₁₉BiN₈: C, 29.75; H, 3.96; N, 23.14. Found: C, 30.14; H, 3.97; N, 23.08.

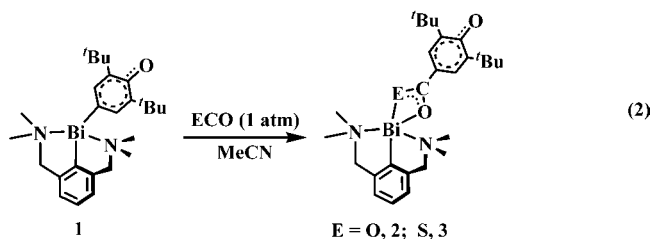
[2,6-(Me₂NCH₂)₂C₆H₃]Bi(N₃)₂, **11**, from Ar'Bi(OC₆H₃Me₂-2,6)₂. Me₃SiN₃ (28 μL, 0.21 mmol) by microsyringe was added to a stirred yellow solution of Ar'Bi(OC₆H₃Me₂-2,6)₂ (55 mg, 0.09 mmol) in THF (5 mL). The yellow color faded and a white precipitate formed over 3 min. Stirring was continued for 1 h and hexane (5 mL) was added. The solid was collected via centrifugation and dried under a vacuum to afford **11** as a white solid (40 mg, 96%) identified by ¹H and ¹³C NMR spectroscopy. (2,6-Dimethylphenoxy)trimethylsilane¹² was isolated and identified as described above in the synthesis of **10**.

Reaction of 1 with Iodine. Addition of a THF (2 mL) solution of iodine (31 mg, 0.12 mmol) to a stirred dark red solution of **1** (74 mg, 0.12 mmol) in THF (8 mL) caused the reaction mixture immediately to become pale yellow in color. Stirring was continued for 1 h, the mixture was filtered, and the solvent was removed from the filtrate. The resulting yellow solid was stirred in hexane (5 mL) for 1 h to extract the organic byproduct. The yellow insoluble material was separated by centrifugation (62 mg) and determined by X-ray crystallography to be Ar'BiI₂.¹ The hexane solution was evaporated under reduced pressure to yield a yellow solid (22 mg) identified by ¹H and ¹³C NMR spectroscopy and GC-MS as the coupled product (3,3',5,5'-tetra-*tert*-butyl-4,4'-diphenylquinone).^{13,14}

X-ray Crystallographic Data. Crystallographic information for complexes **2**, **3**, **8**, **9**, and **11** is summarized in Table 1 and in the Supporting Information.

RESULTS

CO₂ and COS Insertion Reactivity of 1. The red oxyaryl complex, Ar'Bi(C₆H₂^tBu₂-3,5-O-4), **1**, reacts within 1 h with carbon dioxide in acetonitrile to form a yellow product that can be recrystallized from acetonitrile and identified by X-ray crystallography as the oxyarylcarboxy complex Ar'Bi[O₂C(C₆H₂^tBu₂-3-5-O-4)-κ²O,O'], **2**, Figure 1, eq 2. Complex **1**



reacts similarly with carbonyl sulfide (COS) to form the oxyarylthiocarboxy complex Ar'Bi[OSC(C₆H₂^tBu₂-3-5-O-4)-κ²O,S], **3**, Figure 2. Complexes **2** and **3** were also characterized by NMR and IR spectroscopy and elemental analysis. To the best of our knowledge, the reactions in eq 2 are the first examples of insertion of CO₂ and COS into Bi-C bonds.

To examine the generality of the insertion reactivity in eq 2, analogous CO₂ reactions were examined with BiPh₃ and [Ar'Bi(C₆H₂^tBu₂-3,5-OH-4)][BPh₄],⁸ **4**, a molecule that is closely related to **1** in composition and structure, but contains a conventional aryl monoanionic ligand instead of an oxyaryl dianionic ligand. Complex **4** has the same atom connectivity as **1** except that the oxo ligand is protonated and the bond distances are normal for the aryl rings rather than quinoidal (see Figure 3). Neither BiPh₃ nor **4** react with CO₂ under the conditions of eq 2.

Structural Analysis of the Oxyarylcarboxy and Oxyarylthiocarboxy Complexes. X-ray crystallography revealed

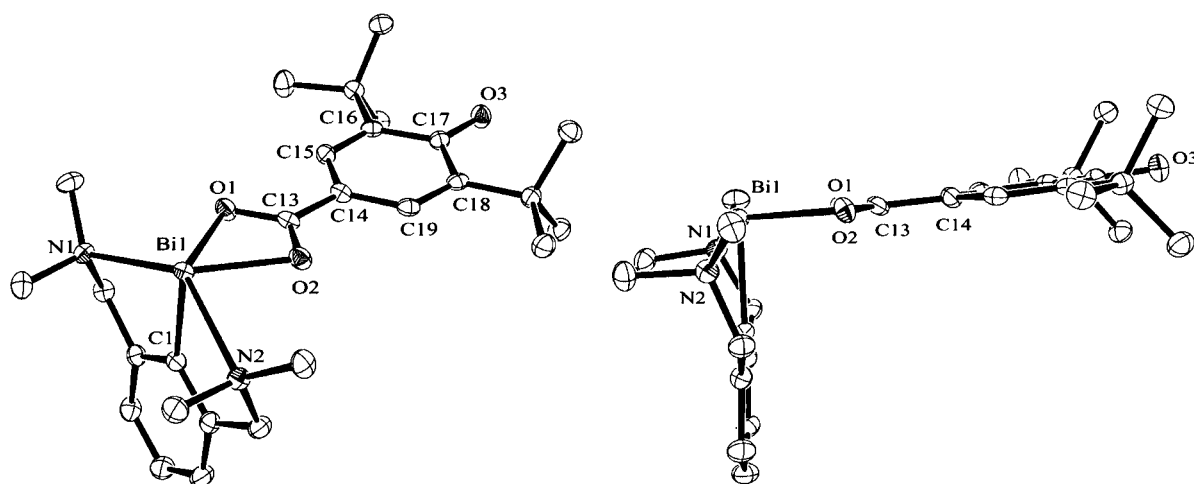


Figure 1. ORTEP¹⁵ representation of Ar'Bi[O₂C(C₆H₂'Bu₂-3-5-O-4)-κ²O,O'], **2**, from two perspectives, with thermal ellipsoids drawn at the 50% probability level. Hydrogen atoms are omitted for clarity.

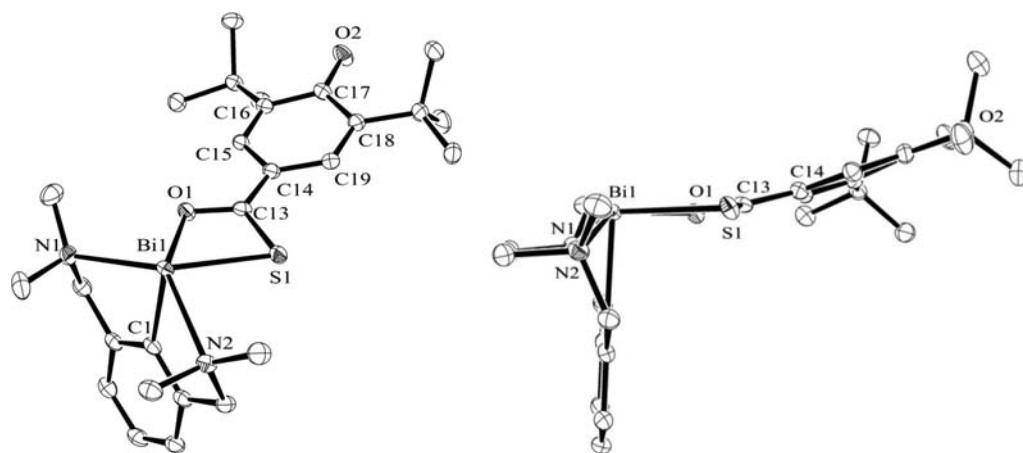


Figure 2. ORTEP representation of Ar'Bi[OSC(C₆H₂'Bu₂-3-5-O-4)-κ²O,S], **3**, from two perspectives, with thermal ellipsoids drawn at the 50% probability level. Hydrogen atoms are omitted for clarity.

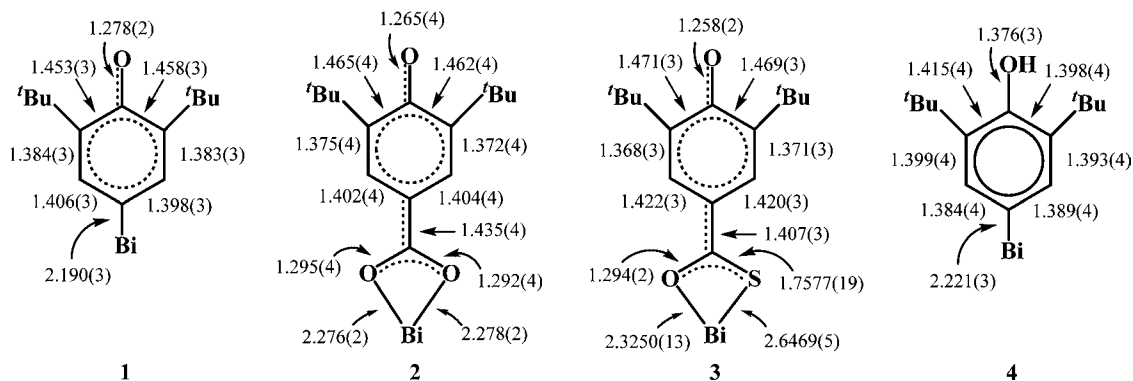


Figure 3. Bond distances in the oxyaryl, oxyarylcarboxy, and oxyarylthiocarboxy dianionic ligands of compounds **1**, **2**, and **3** and the normal bond lengths of the closely related monoanionic hydroxyaryl ligand in **4**.

that **2** and **3** have structures similar to that of **1**. As seen in Figures 1 and 2, complexes **2** and **3** each have their two polydentate ligands oriented at right angles. This provides a large amount of space around the metal as is typical for bismuth.^{1–8,16–19} Complex **1** also has its two ligand planes at 90°, but the orientation differs from that in **2** and **3**. If the Ar' ligand is in the *yz* plane in all three compounds, the dianionic ligands of **2** and **3** are in the *xy* plane, whereas the dianionic

ligand in **1** is in the *xz* plane. The difference occurs presumably to minimize steric interactions between the oxyaryl ring and Ar' since the oxyaryl ring is closer to bismuth in **1**. In **2**, the 178.5(2)° Bi1–C13–C14 angle leads to a 92.4(1)° angle between the Ar' aryl ring and the aryl ring in the dianionic ligand. The analogous angles in **1** are 176.3(2)° and 96.1(1)°. These angles differ in **3**, which has a 167.9(2)° Bi1–C13–C14

angle and a 95.71(6)° angle between the C₆ rings of the two ligands.

The Ar'–Bi moieties of **2** and **3** are conventional like those in **1** and its precursor, Ar'BiCl₂,¹ Table 2. However, the

Table 2. Comparison of Bi–C and Bi–N Distances Involving the Ar' Ancillary Ligand

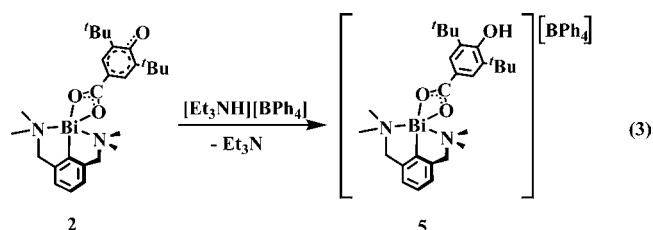
	Bi–C(Ar') (Å)	Bi–N(Ar') (Å)
1	2.208(3)	2.517(3), 2.568(3)
2	2.215(3)	2.542(3), 2.549(3)
3	2.211(2)	2.544(2), 2.619(2)
4	2.202(3)	2.512(2), 2.547(2)
Ar'BiCl ₂	2.224(4) ¹	2.571, 2.561 ¹
BiPh ₃	2.268(8) ³³	

dianionic ligands in **2** and **3** have unusual delocalized bonding as in **1** and in contrast to **4** as shown in Figure 3. For example, the 1.278(2) Å C(17)–O(3) and 1.258(2) Å C(17)–O(2) C–O(oxyaryl) bond distances of **2** and **3**, respectively, are intermediate between single and double bonds (phenol C–O 1.364 Å, quinone C=O 1.220(2) Å²⁰) like the 1.265(4) Å analogue in **1**. The 1.435(4) and 1.407(3) Å C(13)–C(14) distances connecting the aryl ring to the CO₂ and COS carbon atoms in **2** and **3**, respectively, are also both intermediate between single and double bonds. Since the C(15)–C(16) and C(18)–C(19) distances in **2** and **3** are the shortest in the aryl ring like the analogues in **1**, both **2** and **3** have bond distance patterns consistent with quinoidal character. Hence, the structural parameters of the dianionic ligand in **1** are maintained after insertion of CO₂ and COS.

Complexes **2** and **3** are diamagnetic like **1**. However the characteristic splitting of the Ar' protons in the ¹H NMR spectrum of **1**, caused by the asymmetric geometry of the twisted pincer arms, was not observed: only a single set of resonance was observed for the Ar' protons in each case. A resonance for the inserted carboxy carbon atom of **2** was located at 175.8 ppm in the ¹³C NMR spectrum of a ¹³C enriched version of **2**. IR spectroscopy of **2** shows absorptions at 1545 and 1322 cm⁻¹ that fall in the range characteristic of asymmetric and symmetric stretching vibrations for carboxylate ligands.^{21,22} These absorptions shift to 1523 and 1305 cm⁻¹ (Hooke's law calculation: 1512 and 1293 cm⁻¹) in the ¹³C enriched analogue. The IR spectrum of **3** contains absorptions at 1735 and 1597 cm⁻¹, attributable to C–O stretching vibrations that are similar to the 1710–1718 and 1559 cm⁻¹ absorptions of free carbonyl sulfide.²³ An IR absorption at 1019 cm⁻¹ in **3** is in the 934–1043 cm⁻¹ C–S stretching region found in other metal-bound thiocarboxylate ligands.^{24–26}

Protonation of **2** to Form a Carboxyphenol Complex.

The structural uniqueness of the dianionic oxyaryl ligand of **1** was originally defined in part by examining its protonated analogue, [Ar'Bi(C₆H₂^tBu₂-3,5-OH-4)] [BPh₄], **4**, which has normal bond distances in the aryl ring.⁸ A similar comparison was sought for **2**. Addition of [Et₃NH][BPh₄] to **2** yielded a white solid in >85% yield identified as {Ar'Bi[O₂C(C₆H₂^tBu₂-3,5-OH-4)-κ²O,O']}[BPh₄], **5**, by elemental, spectroscopic, and crystallographic analysis, eq 3. The ¹H NMR spectrum of **5** showed resonances typical for Ar' and (BPh₄)¹⁻, as well as a resonance at 6.13 ppm that is consistent with an OH proton. A broad absorption at 3414 cm⁻¹ consistent with an OH group was observed by IR spectroscopy. X-ray crystallography confirmed the atomic connectivity in **5**, but the low quality



of the crystal did not allow detailed discussion of metrical parameters.

Density Functional Theory Analysis of the Oxyarylcarboxy and Oxyarylthiocarboxy Dianionic Ligands. Density functional theory calculations on **2**, **4**, and **5** reveal structural minima that agree very well with the crystallographic data. In the case of **3**, however, the converged calculated structure (Figure S1 in Supporting Information) did not show the upward bend seen in Figure 2. This structural variation may be due to crystal packing. In both **2** and **3**, the new dianionic ligands were found to have delocalized bonding with quinoidal character that was not present in the protonated version of **2**, namely, **5**. An analogous difference was observed in the calculations on **1** and **4**.⁸

The highest occupied molecular orbitals (HOMOs) of **2** and **3** are compared with that of **1** in Figure 4. All three HOMOs

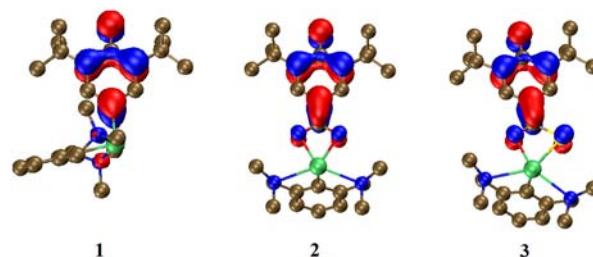
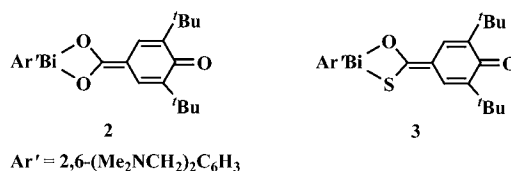


Figure 4. From left to right, HOMO of compounds **1**, **2** and **3**. All orbitals are drawn with a contour value of 0.05.

are similar in the oxy parts of the ligands shown at the top of the figure. The HOMOs of **2** and **3** differ from **1** in the bottom part of the figure. In both **2** and **3**, the HOMO has considerable C=C character between the ipso carbon and the carboxyl or thiocarboxyl carbon. This extends the quinoidal character of the ligands as seen in Scheme 2.

Scheme 2. Quinoidal Resonance Structures of the Dianionic Ligands of Compounds **2** and **3**, Respectively, Showing Double Bond Character



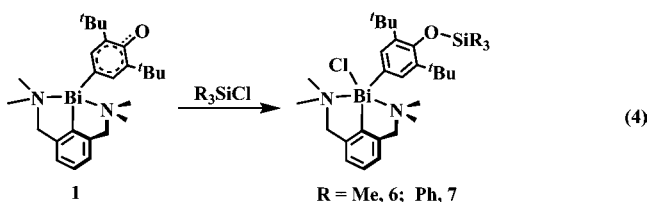
This multiple bonding with the ipso carbon is not found in the HOMO of **1** nor in any other orbitals of **1**: there is only a small interaction between the ipso carbon and bismuth. Hence there is a higher negative charge on the ipso carbon in **1** that correlates with its reactivity with CO₂ and COS.

Natural population analyses (NPA) on **2** and **3** were compared with that of **1** and indicate that insertion of CO₂ and

COS does not significantly affect the electron density on the formally dianionic ligands. In **1**, the oxyaryl ligand has an NPA value of 0.7 electrons, and the analogous numbers for **2** and **3** are 1.0 and 0.8 electrons, respectively. NPA calculations on the ipso carbon of the dianionic ligand showed 4.515 electrons on C13 of **1** compared to 4.224 and 4.183 electrons for C14 of the oxyarylcarboxy and oxyarylthiocarboxy dianionic ligands of **2** and **3**, respectively. The higher electron density on C13 in **1** is spread out to the carboxyl and thiocarboxyl groups in **2** and **3** so that C14 in those compounds has lower electron density. The electron density on C13 in **1** is also higher than the 4.435 and 4.347 values on the analogous carbons in the protonated conventional aryl complex, **4**, and BiPh₃, respectively. This difference can be used to rationalize the CO₂ and COS insertion reactivity observed for **1** and not for **4** and BiPh₃.

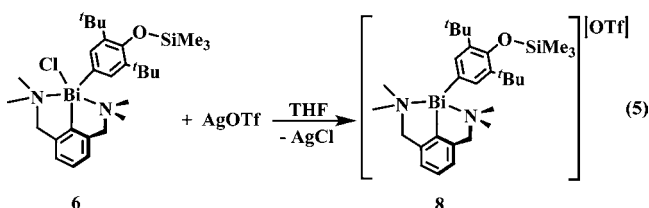
Reactions of **1** with Silyl Halides and Pseudohalides.

Complex **1** reacts with 1 equiv of trimethylsilyl chloride to form Ar'BiCl(C₆H₂^tBu₂-3,5-OSiMe₃-4), **6**, in over 85% yield as shown in eq 4. Ph₃SiCl reacts similarly to form Ar'BiCl-



(C₆H₂^tBu₂-3,5-OSiPh₃-4), **7**, in over 65% yield. These reactions constitute formal addition of R₃SiCl over five bonds. NMR spectroscopy and elemental analytical data are consistent with the compounds as formulated, but crystallographic confirmation of these compounds has been elusive.

In order to further explore the nature of these silylated products and in an attempt to derivatize **6** to crystallographically characterize an example of a Ar'Bi(monooanion)-(C₆H₂^tBu₂-3,5-OSiR₃-4) complex, **6** was treated with 1 equiv of AgOTf (OTf = CF₃SO₃⁻). A precipitate consistent with AgCl formed, and the desired triflate derivative was isolated, eq 5.



Although chloride in **6** was replaced by the triflate, X-ray crystallography showed that the complex crystallized as an outer sphere triflate complex, i.e. [Ar'Bi(C₆H₂^tBu₂-3,5-OSiMe₃-4)][CF₃SO₃], **8**, Figure 5. The ¹H NMR spectrum of compound **6** shows a single broad peak for the NMe₂ protons of Ar', while compound **8** has two singlets similar to that seen for **1**. This difference may arise because the triflate ligand in **8** is outer sphere, while **6** may have the chloride ligand coordinated to the metal center.

Structural evidence for the Ar'Bi(X)(C₆H₂^tBu₂-3,5-OSiR₃-4) products in eq 4 in which X was coordinated to bismuth was obtainable by examining the reaction of **1** with the trimethylsilyl pseudohalide, Me₃SiCN. The reaction of **1** with Me₃SiCN in one case formed single crystals of the 1,5-addition product, namely, Ar'Bi(CN)(C₆H₂^tBu₂-3,5-OSiMe₃-4), **9**, that could be characterized by X-ray crystallography, Figure 6. Although **9**

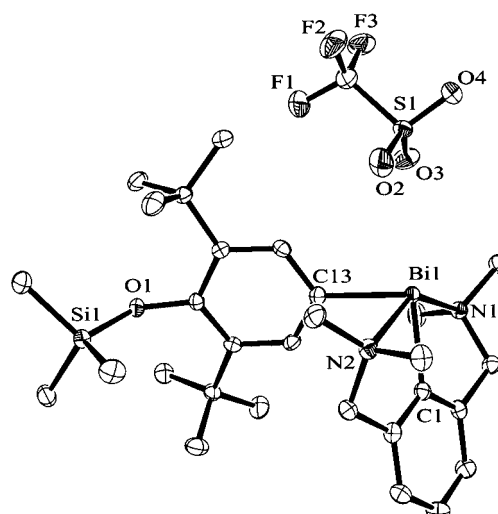


Figure 5. ORTEP representation of [Ar'Bi(C₆H₂^tBu₂-3,5-OSiMe₃-4)][CF₃SO₃], **8**, with thermal ellipsoids drawn at the 50% probability level. Hydrogen atoms are omitted for clarity.

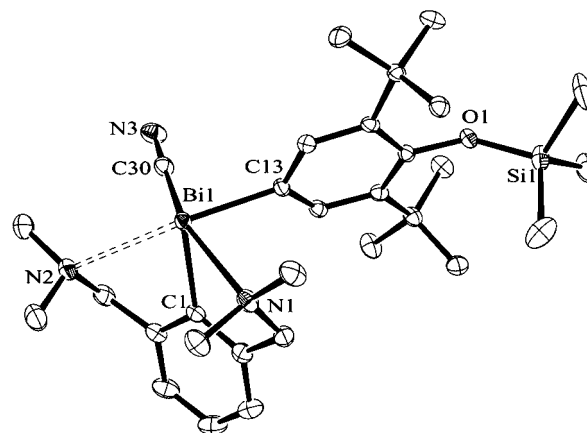
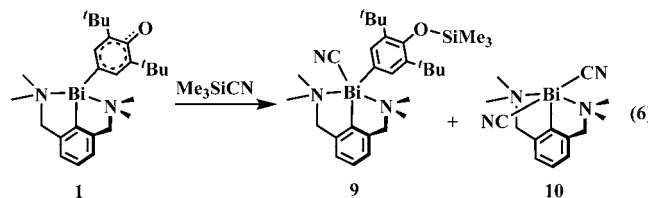


Figure 6. ORTEP representation of Ar'Bi(CN)(C₆H₂^tBu₂-3,5-OSiMe₃-4), **9**, with thermal ellipsoids drawn at the 50% probability level. Hydrogen atoms are omitted for clarity.

provided a desired structural example, it was not the main product of the Me₃SiCN reaction. The predominant and most commonly obtained product of the reaction was the dicyanide complex, Ar'Bi(CN)₂, **10**, eq 6. Single crystals of **10** were analyzed by X-ray crystallography, but a structure solution was not obtainable, possibly because of disorder.



The formation of Ar'BiX₂ products from R₃SiX reactions with **1** as observed for **9** and **10** in eq 6 appears to be general. With Me₃SiN₃, NMR evidence for the initial 1,5-addition product, Ar'Bi(N₃)(C₆H₂^tBu₂-3,5-OSiMe₃-4) is observed, but the main product is Ar'Bi(N₃)₂, **11**. In contrast to **10**, this complex can be crystallographically characterized as shown in

Figure 7. Metrical parameters on **8**, **9**, and **11** are presented in the Supporting Information.

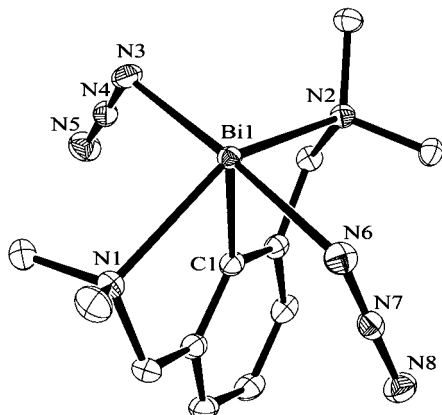
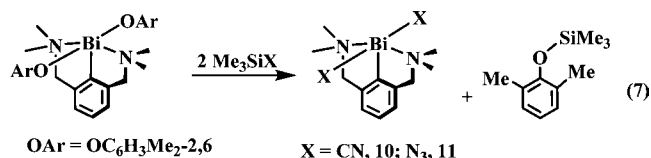
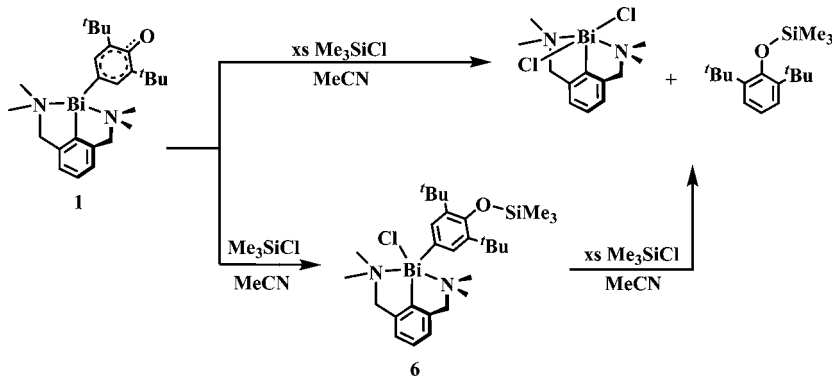


Figure 7. ORTEP representation of $\text{Ar}'\text{Bi}(\text{N}_3)_2$, **11**, with thermal ellipsoids drawn at the 50% probability level. Hydrogen atoms were omitted for clarity.

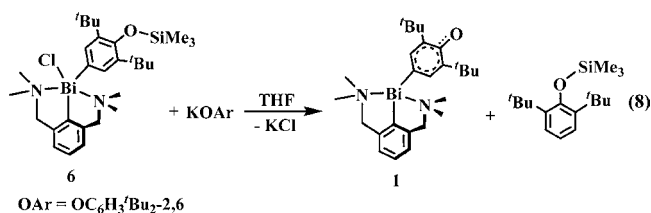
$\text{Ar}'\text{BiX}_2$ products are also obtainable from R_3SiX reactions with **1** when $\text{X} = \text{Cl}$. When **1** is reacted with an excess of Me_3SiCl , the known dichloride, $\text{Ar}'\text{BiCl}_2$,¹ is formed quantitatively along with the silyl ether $\text{Me}_3\text{SiOC}_6\text{H}_3^t\text{Bu}_2$,¹⁰ which was identified by ^1H NMR spectroscopy and GC–MS, Scheme 3. This reaction can also be done stepwise: addition of Me_3SiCl to the initial reaction product, **6**, also generates $\text{Ar}'\text{BiCl}_2$ and $\text{Me}_3\text{SiOC}_6\text{H}_3^t\text{Bu}_2$. The isolation of this silyl ether indicates that the $[(\text{C}_6\text{H}_2^t\text{Bu}_2\text{-3,5-O-SiMe}_3\text{-4})]^{1-}$ unit in **6** has added hydrogen. When the reaction of **1** with excess Me_3SiCl was performed in CD_3CN , ^2H NMR spectroscopy and GC–MS indicated that the ether product contained deuterium on the carbon atom previously attached to bismuth, i.e., $\text{Me}_3\text{SiOC}_6\text{H}_2^t\text{Bu}_2\text{-2,6-D-4}$. Hence, solvent can be the source of hydrogen or deuterium.

To aid in NMR analysis of the complicated mixtures of $\text{Ar}'\text{Bi}(\text{X})(\text{C}_6\text{H}_2^t\text{Bu}_2\text{-3,5-O-SiMe}_3\text{-4})$ and $\text{Ar}'\text{BiX}_2$ formed from reactions of Me_3SiX with **1**, $\text{Ar}'\text{Bi}(\text{N}_3)_2$ and $\text{Ar}'\text{Bi}(\text{CN})_2$ were independently synthesized by treatment of the previously reported bis(aryloxide) $\text{Ar}'\text{Bi}(\text{OC}_6\text{H}_3\text{Me}_2\text{-2,6})_2$ ⁸ with excess Me_3SiX reagent ($\text{X} = \text{N}_3$ and CN), eq 7. The byproduct from these reactions is the expected silyl ether, $\text{Me}_3\text{SiOC}_6\text{H}_3\text{Me}_2\text{-2,6}$,¹² as confirmed by ^1H NMR spectroscopy and GC–MS.

Scheme 3. Direct Synthesis of $\text{Ar}'\text{BiCl}_2$ and $\text{Me}_3\text{SiOC}_6\text{H}_3^t\text{Bu}_2$,⁶ by **1** and Excess Me_3SiCl and Step-Wise Synthesis through Compound **6**

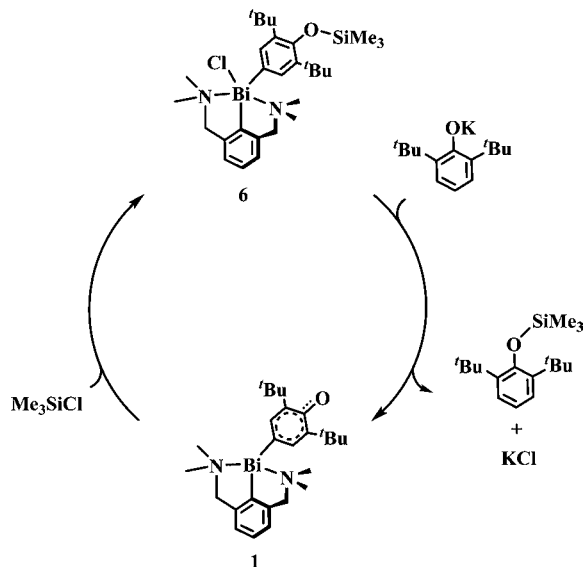


Regeneration of the Dianionic Oxyaryl Ligand from $\text{Ar}'\text{BiCl}(\text{C}_6\text{H}_2^t\text{Bu}_2\text{-3,5-O-SiMe}_3\text{-4})$, **6.** The reaction of **6** with 1 equiv of $\text{KOC}_6\text{H}_3^t\text{Bu}_2$,⁶ does not lead to a simple substitution of chloride in a reaction analogous to that observed with AgOTf in eq 5. Instead, the aryloxide reaction regenerates the dianionic oxyaryl ligand, $(\text{C}_6\text{H}_2^t\text{Bu}_2\text{-3,5-O})^{2-}$, and compound **1** with formation of the silyl ether $\text{Me}_3\text{SiOC}_6\text{H}_3^t\text{Bu}_2$,⁶ and KCl , eq 8.



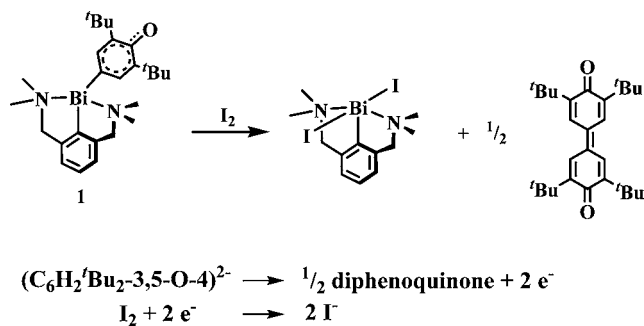
The reaction pathway initially considered for eq 8 was a radical process involving an $\text{Ar}'\text{Bi}[\text{OC}_6\text{H}_3^t\text{Bu}_2\text{-2,6}](\text{C}_6\text{H}_2^t\text{Bu}_2\text{-3,5-O-SiMe}_3\text{-4})$ intermediate that would undergo Bi-O homolysis as proposed for the synthesis of **1**.⁸ This possibility was tested with the analogous reaction of **6** with a *para*-methyl-substituted aryloxide, $\text{KOC}_6\text{H}_2^t\text{Bu}_2\text{-2,6-Me-4}$. With the *para* position substituted, this phenolate cannot form the aryl radical necessary in the radical pathway.⁸ However, the reaction of **6** with $\text{KOC}_6\text{H}_2^t\text{Bu}_2\text{-2,6-Me-4}$ also immediately gives the characteristic color change to dark red for the formation of **1**. Complex **1** is indeed formed in this reaction and the byproduct silyl ether was identified as (2,6-di-*tert*-butyl-4-methylphenoxy)-trimethylsilane¹¹ by ^1H NMR spectroscopy and GC–MS. It is therefore more likely that the reaction of **6** with a phenolate follows a less complex mechanism, Scheme 4, in which the nucleophilic phenolate abstracts the Me_3Si group with concomitant KCl formation. This mechanism is consistent with the experimental observations.

Interestingly, the addition of $\text{KOC}_6\text{H}_3^t\text{Bu}_2$,⁶ to the chloride complex, **6**, leads to regeneration of **1** in a cyclic process, Scheme 5, that involves the net conversion of $\text{KOC}_6\text{H}_3^t\text{Bu}_2$,⁶ and Me_3SiCl to $\text{Me}_3\text{SiOC}_6\text{H}_3^t\text{Bu}_2$,⁶ and KCl . Although this

Scheme 4. Possible Mechanism for Me₃Si Abstraction and the Reformation of 1 from 6 and KOC₆H₂^tBu₂-2,6-Me-4Scheme 5. Cyclic Synthesis of the Silyl Ether (2,6-Di-*tert*-butylphenyl)(trimethylsilyl)ether

particular transformation is not difficult to effect by other means, the reactions in Scheme 5 show that bismuth and the oxyaryl dianionic ligand can participate in cyclic reaction chemistry.

Reaction of 1 with Iodine. The reaction of 1 with I₂ in THF affords Ar'BiI₂,¹ analogous to the Ar'BiX₂ species formed in eq 6 and Scheme 3, but the coproduct is 3,3',5,5'-tetra-*tert*-butyl-4,4'-diphenquinone,^{13,14} Scheme 6. The diphenoqui-

Scheme 6. Reaction of 1 with I₂ to Form the Coupled Product 3,3',5,5'-Tetra-*tert*-butyl-4,4'-diphenquinone

none, identified by ¹H and ¹³C NMR spectroscopy and by GC–MS, is a common byproduct in bismuth aryloxy chemistry and has been isolated from reactions of BiCl₃ and 3 equiv of LiOC₆H₃^tBu₂-2,6 by Hanna and co-workers in a process thought to involve Bi–O bond homolysis.^{27,28} The reaction formally involves the two electron oxidation of the oxyaryl dianionic ligand by iodine as shown by the half

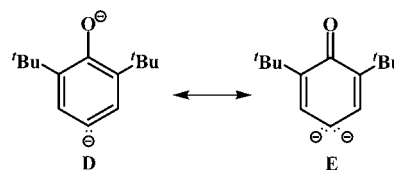
reactions, but the mechanism of the transformation is unknown.

DISCUSSION

Although CO₂ insertion into metal–carbon bonds is a characteristic organometallic reaction for most metals,^{21,29,30} it is not as common with main group metals.³¹ To our knowledge, the reactions of CO₂ and COS with the oxyaryl complex Ar'Bi(C₆H₂^tBu₂-3,5-O-4), 1, are the first examples of insertion of these substrates into Bi–C bonds. The fact that CO₂ does not react with BiPh₃ and the aryl monoanion complex [Ar'Bi(C₆H₂^tBu₂-3,5-OH-4)][BPh₄],⁸ 4, that is closely related to 1, indicates that this reactivity arises from the special electronic nature of the dianionic oxyaryl ligand.

The enhanced reactivity of the oxyaryl ligand in 1 can be rationalized with the resonance structures in Scheme 7.

Scheme 7. Two Resonance Structures for the Oxyaryl Dianionic Ligand of Compound 1

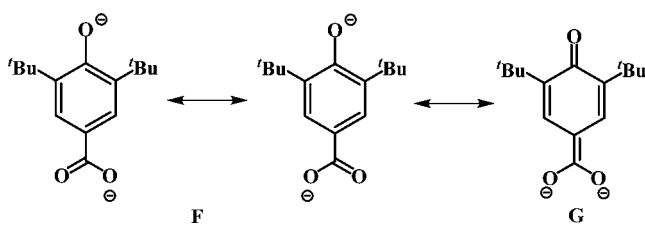


Resonance form D matches that expected in conventional Bi–C(aryl) complexes that do not insert CO₂. However, quinoidal resonance structure E has enhanced negative charge at the *para*-carbon position that could lead to the observed reactivity with CO₂ and COS. Since the bond distances in 1 are in between those expected for D and E, structure E can be a significant contributor to reactivity. The higher charge at this *para*-carbon is not significantly stabilized by bismuth, as shown by the DFT calculations, Figure 4, and hence this carbon is thus more reactive than those in typical organobismuth complexes. Since the oxyaryl dianionic ligand is known only in 1, comparisons of its reactivity attached to other metals cannot be made.

Insertion of CO₂ and COS into the Bi–C bond of 1 generates two new dianionic ligands, [O₂C(C₆H₂^tBu₂-3,5-O-4)-κ²O,O']²⁻ and [OSC(C₆H₂^tBu₂-3,5-O-4)-κ²O,S]²⁻, both of which also show delocalized bonding as in the [C₆H₂^tBu₂-3,5-O-4]²⁻ dianion in 1. In the quinoidal resonance forms of these dianionic ligands, the –2 charge localized on the *para*-carbon in 1 (Structure E above) can be spread over three additional atoms as shown in Scheme 8.

The reactivity of 1 with R₃SiCl, eq 4, can be rationalized by resonance structure D in Scheme 7. The anionic phenolate oxygen in that resonance form could be sufficiently nucleophilic to react with a trimethylsilyl group to form a strong Si–O bond. This would create a transient cationic species, [Ar'Bi(C₆H₂^tBu₂-3,5-O-SiR₃-4)]⁺, with an outer sphere X[–] counteranion that could subsequently coordinate to bismuth to make 6

Scheme 8. Possible Resonance Structures of the Oxyarylcarboxy Dianionic Ligand of Compound 2



or 7. The synthesis of the outer sphere triflate salt, $[\text{Ar}'\text{Bi}(\text{C}_6\text{H}_2^t\text{Bu}_{2-3,5}\text{-OSiMe}_3\text{-4})][\text{CF}_3\text{SO}_3]$, **8**, shows that such cations can exist with the appropriate counteranion. These reactions are analogous to the protonation of **2** to make $\{\text{Ar}'\text{Bi}[\text{OC}(\text{C}_6\text{H}_2^t\text{Bu}_{2-3,5}\text{-OH-4})\text{O-}\kappa^2\text{O,O}']\}[\text{BPh}_4]$, **5**, eq 4. The net result of nucleophilic attack on Me_3SiX reagents followed by capture of X^- by bismuth is formal addition of Si-X over five bonds.

The reaction of excess R_3SiX with **1** to produce $\text{Ar}'\text{BiX}_2$, e.g., eq 6, and the stepwise reaction of $\text{Ar}'\text{BiCl}(\text{C}_6\text{H}_2^t\text{Bu}_{2-3,5}\text{-OSiMe}_3\text{-4})$, **6**, with Me_3SiCl to make $\text{Ar}'\text{BiCl}_2$, Scheme 3, are consistent with the stability of $\text{Ar}'\text{BiX}_2$ complexes as end products. $\text{Ar}'\text{BiX}_2$ complexes are commonly observed in reactions involving the $[\text{Ar}'\text{Bi}]^{2+}$ moiety.^{2,17–19} The formation of the silyl ether product of this reaction, $\text{R}_3\text{SiOC}_6\text{H}_3^t\text{Bu}_{2-2,6}$, is consistent with the hydrogen abstraction chemistry frequently found in bismuth reactions.³² In CD_3CN , the hydrogen (deuterium) was found to originate from solvent.

Attempts to obtain structural data on the bismuth complexes in this study reveal some unexpected irregularities in the ability to obtain single crystals suitable for crystallography. For example, although $\text{Ar}'\text{BiCl}_2^1$ and $\text{Ar}'\text{Bi}(\text{OAr})_2$ ($\text{OAr} = [\text{OC}_6\text{H}_3\text{Me}_{2-2,6}]^{1-}$, $[\text{OC}_6\text{H}_3\text{Pr}_{2-2,6}]^{1-}$, $[\text{OC}_6\text{H}_2^t\text{Bu}_{2-2,6}\text{-Me-4}]^{1-}$)⁸ readily crystallize, the $\text{X} = \text{Cl}$ version of the $\text{Ar}'\text{Bi}(\text{X})(\text{C}_6\text{H}_2^t\text{Bu}_{2-3,5}\text{-OSiR}_3\text{-4})$ series did not. Instead, the $\text{X} = \text{CN}$ derivative gave good single crystals of this structural type even though it is difficult to isolate this compound compared to the main product of the reaction, $\text{Ar}'\text{Bi}(\text{CN})_2$. The latter dicyanide did not give good crystal data in contrast to $\text{Ar}'\text{BiCl}_2^1$ and $\text{Ar}'\text{Bi}(\text{N}_3)_2$, which did give solvable data. Although complexes **1** and **2** both crystallize to provide good data, their protonated analogues **4** and **5**, respectively, differed. Only for **4** was crystallographically acceptable data obtained. No patterns emerge from these data, but they do suggest that slight modification of components in $[\text{Ar}'\text{Bi}]^{2+}$ complexes may lead to crystallographically definable derivatives of new compounds.

CONCLUSION

The quinoidal character of the unusual oxyaryl dianionic ligand, $(\text{C}_6\text{H}_2^t\text{Bu}_{2-3,5}\text{-O-4})^{2-}$, in the Bi^{3+} complex $\text{Ar}'\text{Bi}(\text{C}_6\text{H}_2^t\text{Bu}_{2-3,5}\text{-O-4})$, **1**, has led to the first insertion reactions of CO_2 and COS into Bi-C bonds. These reactions generate new dianionic ligands with quinoidal character, $[\text{O}_2\text{C}(\text{C}_6\text{H}_2^t\text{Bu}_{2-3,5}\text{-O-4})\text{-}\kappa^2\text{O,O}']^{2-}$ and $[\text{OSC}(\text{C}_6\text{H}_2^t\text{Bu}_{2-3,5}\text{-O-4})\text{-}\kappa^2\text{O,S}]^{2-}$ in **2** and **3**, respectively. Reactions of **1** with silyl halides and pseudohalides Me_3SiX ($\text{X} = \text{Cl}, \text{CN}, \text{N}_3$) lead to formal addition of Si-X across five bonds to form $\text{Ar}'\text{Bi}(\text{X})(\text{C}_6\text{H}_2^t\text{Bu}_{2-3,5}\text{-OSiMe}_3\text{-4})$ complexes. These react with additional Me_3SiX to generate $\text{Ar}'\text{BiX}_2$ complexes and (2,6-di-*tert*-butylphenyl)(trimethylsilyl)ether. Addition of $\text{KOC}_6\text{H}_3^t\text{Bu}_{2-2,6}$ to $\text{Ar}'\text{Bi}(\text{Cl})(\text{C}_6\text{H}_2^t\text{Bu}_{2-3,5}\text{-OSiMe}_3\text{-4})$ regenerates **1** in a cyclic process

that converts $\text{KOC}_6\text{H}_3^t\text{Bu}_{2-2,6}$ and Me_3SiCl to $\text{Me}_3\text{SiOC}_6\text{H}_3^t\text{Bu}_{2-2,6}$ and KCl using the bismuth complex in a cyclic fashion to facilitate the transformation.

ASSOCIATED CONTENT

Supporting Information

Computational details, selected bond distances, converged calculated structure for **3**, and crystallographic data (CIF) for **2**, **3**, **8**, **9**, and **11**. This material is available free of charge via the Internet at <http://pubs.acs.org>. CCDC 931429 (**8**), 931430 (**3**), 931431 (**9**), 931432 (**11**), and 931433 (**2**) contains the supplementary crystallographic data for this paper. These data can be obtained free of charge from The Cambridge Crystallographic Data Centre via www.ccdc.cam.ac.uk/data_request/cif.

AUTHOR INFORMATION

Corresponding Author

wevans@uci.edu

Notes

The authors declare no competing financial interest.

ACKNOWLEDGMENTS

We thank the Chemical Sciences, Geosciences, and Biosciences Division of the Office of Basic Energy Sciences of the Department of Energy (DE-FG03-86ER13514 to W.J.E.) and the U.S. National Science Foundation (CHE-1213382 to F.F.) for financial support of this work. We also thank Ryan A. Zarkesh and Jordan F. Corbey for assistance with X-ray crystallography.

REFERENCES

- (1) Soran, A. P.; Silvestru, C.; Breunig, H. J.; Balázs, G.; Green, J. C. *Organometallics* **2007**, *26*, 1196.
- (2) Soran, A.; Breunig, H. J.; Lippolis, V.; Arca, M.; Silvestru, C. *Dalton Trans.* **2009**, *38*, 77.
- (3) Breunig, H. J.; Nema, M. G.; Silvestru, C.; Soran, A. P.; Varga, R. A. *Dalton Trans.* **2010**, *39*, 11277.
- (4) Casely, I. J.; Ziller, J. W.; Mincher, B. J.; Evans, W. J. *Inorg. Chem.* **2011**, *50*, 1513.
- (5) Mairychová, B.; Svoboda, T.; Štěpnička, P.; Růžička, A.; Havenith, R. W. A.; Alonso, M.; Proft, F. D.; Jambor, R.; Dostál, L. *Inorg. Chem.* **2013**, *52*, 1424.
- (6) Mairychová, B.; Svoboda, T.; Erben, M.; Růžička, A.; Dostál, L.; Jambor, R. *Organometallics* **2013**, *32*, 157.
- (7) Šimon, P.; Jambor, R.; Růžička, A.; Dostál, L. *Organometallics* **2013**, *32*, 239.
- (8) Casely, I. J.; Ziller, J. W.; Fang, M.; Furche, F.; Evans, W. J. *J. Am. Chem. Soc.* **2011**, *133*, 5244.
- (9) Boyle, T. J.; Andrews, N. L.; Rodriguez, M. A.; Campana, C.; Yiu, T. *Inorg. Chem.* **2003**, *42*, 5357.
- (10) Goyal, M.; Singh, A. *Main Group Met. Chem.* **1996**, *19*, 587.
- (11) Healy, M. D.; Barron, A. R. *J. Organomet. Chem.* **1990**, *381*, 165.
- (12) Yasuda, H.; Nakayama, Y.; Takei, K.; Nakamura, A.; Kai, Y.; Kanehisa, N. *J. Organomet. Chem.* **1994**, *473*, 105.
- (13) Liao, B.; Liu, Y.; Peng, S.; Liu, S. *Dalton Trans.* **2012**, *41*, 1158.
- (14) Astolfi, P.; Panagiotaki, M.; Greci, L. *Eur. J. Org. Chem.* **2005**, *14*, 3052.
- (15) Burnett, M. N.; Johnson, C. K. *ORTEP-III: Oak Ridge Thermal Ellipsoid Plot Program for Crystal Structure Illustrations*; Oak Ridge National Laboratory: Oak Ridge, TN, 1996; Report ORNL-6895.
- (16) Norman, N. C. *Chemistry of Arsenic, Antimony, and Bismuth*; Blackie Academic and Professional: London, 1998; Chapter 1.
- (17) Atwood, D. A.; Cowley, A. H.; Ruiz, J. *Inorg. Chim. Acta* **1992**, *198–200*, 271.

- (18) Breunig, H. J.; Königsman, L.; Lork, E.; Nema, M.; Philipp, N.; Silvestru, C.; Soran, A.; Varga, R. A.; Wagner, R. *Dalton Trans.* **2008**, 37, 1831.
- (19) Silvestru, C.; Breunig, H. J.; Althaus, H. *Chem. Rev.* **1999**, 99, 3277.
- (20) Allen, F. H.; Kennard, O.; Watson, D. G.; Brammer, L.; Orpen, A. G.; Taylor, R. J. *Chem. Soc., Perkin Trans. 2* **1987**, 12, S1.
- (21) Gibson, D. H. *Chem. Rev.* **1996**, 96, 2063.
- (22) Bellamy, L. J. *The Infra-red Spectra of Complex Molecules*; John Wiley & Sons, Inc.: New York, 1964.
- (23) Ferm, R. J. *Chem. Rev.* **1957**, 57, 621.
- (24) Hans, M.; Willem, Q.; Wouters, J.; Demonceau, A.; Delaude, L. *Organometallics* **2011**, 30, 6133.
- (25) Contreras, L.; Láinez, R. F.; Pizzano, A.; Sánchez, L.; Carmona, E. *Organometallics* **2000**, 19, 261.
- (26) Chaturvedi, J.; Singh, S.; Bhattacharya, S.; Nöth, H. *Inorg. Chem.* **2011**, 50, 10056.
- (27) Hanna, T. A.; Rieger, A. L.; Rieger, P. H.; Wang, X. *Inorg. Chem.* **2002**, 41, 3590.
- (28) Kou, X.; Wang, X.; Mendoza-Espinosa, D.; Zakharov, L. N.; Rheingold, A. L.; Watson, W. H.; Brien, K. A.; Javarathna, L. K.; Hanna, T. A. *Inorg. Chem.* **2009**, 48, 11002.
- (29) Braunstein, P.; Matt, D.; Nobel, D. *Chem. Rev.* **1988**, 88, 747.
- (30) Omae, I. *Coord. Chem. Rev.* **2012**, 256, 1384.
- (31) Mömning, C. M.; Otten, E.; Kehr, G.; Fröhlich, R.; Grimme, S.; Stephan, D. W.; Erker, G. *Angew. Chem., Int. Ed.* **2009**, 48, 6643.
- (32) Hanna, T. A. *Coord. Chem. Rev.* **2004**, 248, 429.
- (33) Jones, P. G.; Blaschette, A.; Henschel, D.; Weitze, A. Z. *Kristallogr.* **1995**, 210, 377.